NANO LETTERS

Letter

pubs.acs.org/NanoLett

Signal-to-Noise Ratio Enhancement of Silicon Nanowires Biosensor with Rolling Circle Amplification

Anran Gao,† Nengli Zou,† Pengfei Dai, Na Lu, Tie Li,* Yuelin Wang,* Jianlong Zhao, and Hongju Mao*

State Key Laboratories of Transducer Technology & Science and Technology on Micro-system Laboratory, Shanghai Institute of Microsystem and Information Technology, Chinese Academy of Sciences, Shanghai, 200050, China

Supporting Information

ABSTRACT: Herein, we describe a novel approach for rapid, label-free and specific DNA detection by applying rolling circle amplification (RCA) based on silicon nanowire field-effect transistor (SiNW-FET) for the first time. Highly responsive SiNWs were fabricated with a complementary metal oxide semiconductor (CMOS) compatible anisotropic self-stop etching technique which eliminated the need for hybrid method. The probe DNA was immobilized on the surface of SiNW, followed by sandwich hybridization with the perfectly matched target DNA and RCA primer that acted as a primer to hybridize the RCA template. The RCA reaction created a long single-stranded DNA (ssDNA) product and thus enhanced the electronic responses of SiNW significantly. The signal-to-noise ratio (SNR) as a figure-of-merit was analyzed to estimate the signal enhancement and possible detection limit. The nanosensor showed highly sensitive concentration-dependent conductance change in response to specific target DNA sequences. Because of the binding of an abundance of repeated sequences of RCA products, the SNR of >20 for 1 fM DNA detection was achieved, implying a detection floor of 50 aM. This RCA-based SiNW biosensor also discriminated perfectly matched target DNA from one-base mismatched DNA with high selectivity due to the substantially reduced nonspecific binding onto the SiNW surface through RCA. The combination of SiNW FET sensor with RCA will increase diagnostic capacity and the ability of laboratories to detect unexpected viruses, making it a potential tool for early diagnosis of gene-related diseases.

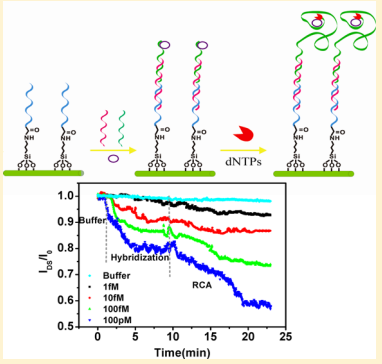

KEYWORDS: *SiNW-FETs, rolling circle amplification, biosensor, DNA detection, ultrasensitive*

As the carriers of genetic information in all cells and in many viruses, nucleic acids store most of the genetic information for almost every specimen and are involved in all growth and developmental processes of these organisms.[1,2] The novel methods for sensitive, specific, reliable, and repaid detection of nucleic acid are therefore highly desired for molecular biology research[3−5] and disease diagnosis[6−8] especially in the early diagnosis of a variety of infectious and hereditary diseases, such as Hepatitis B, an exogenous gene expression infectious disease. The copy number and genotype of Hepatitis B virus (HBV) DNA are very closely related to the disease progression and infection of Hepatitis B patients,[9,10] which makes the quantitative detection of low-abundance DNA very useful in the treatment and prevention of HBV or some other infectious diseases. In detecting small amounts of specific molecules, it is of great importance to convert the biological information into an electronic signal. Several reported methods including nanoparticles,[11] cantilever,[12] carbon nanotubes,[13] and so on cannot satisfy the demand of repaid, highly sensitive and selective biochemical detection. Semiconducting nanowire (NW) as biosensor has received considerable attention because of its sensitivity, selectivity, label-free, and real-time detection capabilities.[14,15] By exploiting these attractive properties, semiconducting NWs have been designed for recognizing a wide range of targets.[14,16−18]

A variety of potential noise sources is crucial for NW biosensing applications including intrinsic device noise due to mobility and/or carrier fluctuations,[19] thermal fluctuations of the environment,[20] and the interaction between biomolecules and the NW surface.[21] NWs-based biosensor is liable to the interference thus has a high demand for testing environment and circuit.[22] The signal of SiNW is typically very weak, variable, and not dependent on the target molecule concentration especially for ultralow concentrations of the target because of fluctuations in the signal.[22] Therefore, in order to simplify the testing circuit, lower the cost, improve detection ability, and thus result in a more robust and portable device, the improvement in signal-to-noise ratio (SNR) level of NW device is imperative. The SNR will also determine the sensitivity limit of the biosensor,[23] which is expected to be improved naturally. Better detection limit will increase capacity of clinical diagnosis because of the ultralow concentrations of specific markers in clinical samples. However, to date NW FET biosensor studies have focused primarily on measuring the total signal, such as silicon nanowire (SiNW) FET conductance, as a function of changes in the analyte concentration.[24,25] SNR in

Received: May 4, 2013
Revised: August 3, 2013

dx.doi.org/10.1021/nl401628y | *Nano Lett.* XXXX, XXX, XXX−XXX

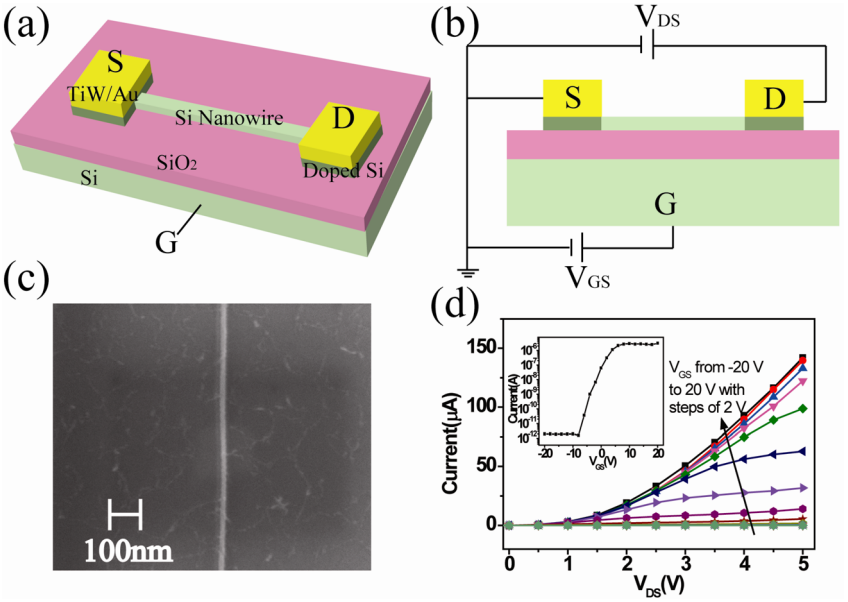

Figure 1. Device fabrication and electrical performance. (a) The schematic diagram of a completed SiNW FET. The source (S), drain (D), and underlying back-gate (G) are labeled. (b) The cross-sectional view of a nanowire with gate potential and source/drain bias voltage labeled. (c) Scanning electron micrograph of a typical SiNW with width of about 20 nm. (d) I_{DS}/V_{DS} curve for varying V_{GS} (−20 to 20 V, ΔV = 2 V), illustrating n-type accumulation mode behavior and I_{DS}/V_{GS} curve for V_{DS} = 1 V (inset) of nanowire with length of 6 μm.

the SiNW FET device at equilibrium have not, however, been studied too much.

In order to improve the SNR of NW device, it is not only necessary to reduce the noise level but also to have a high gain in order to provide a high SNR, thus also preventing the high number of false positive and false negative incidents. Therefore, additional target signal enhancement is necessary in order to detect minute concentrations of targets especially in cases where the extrinsic noise level is high. Willner et al. have performed some pioneering study on amplified sensing of DNA by the application of enzymes,[26] nanoparticles,[27,28] and magnetic particles,[29] which provides guidance for our work. The most commonly used methods include polymerase chain reaction (PCR),[30] T7 polymerase amplification,[31] and rolling circle amplification (RCA).[32,33] PCR is usually used to amplify defined sequences, but the introduction sequence errors and the requirements for thermal cycling have limited its applicability in nucleic acid detection. RCA is a simple and unique amplification method with high sensitivity and specificity owing to the stringent strand matching requirement and its high amplification efficiency.[32] In addition, unlike T7 polymerase amplification procedure RCA produces a signal amplified product that remains linked to the DNA primer and hence the method is suited to solid phase formats such as SiNW-FET for generating localized signal at specific location.[33] Being an isothermal process, RCA also overcomes the need for costly and cumbersome equipment for temperature cycling and reduces the complexity of the biosensor. Nevertheless, RCA combined with various methods, such as electrochemical, fluorescence chemiluminescence and bioluminescence, and so on, are typically label-dependent with complex steps and comparatively low sensitivity.[32,34−37]

Herein, we developed a new approach for sensitive and specific HBV DNA detection by the combination of silicon nanowire with RCA. The method that could result in signal enhancement, eliminate expensive labeling steps, and simplify signal readout was described for the first time. It also facilitated object analysis, reduced the number of false counts, and resulted in a more robust protocol. The signal was significantly amplified due to the binding of an abundance of repeated sequences of RCA products. The SNR of SiNW was analyzed intensively to provide guidance for the design and optimization of silicon nanowire sensor. Hence, the direct and label-free detection of HBV DNA with SNR > 20 for DNA concentration down to 1 fM and high specificity for single-nucleotide polymorphism (SNP) discrimination were achieved. The combination of SiNW FET sensor with RCA will not only increase diagnostic capacity but also have potential in real-time single-molecule detection.

Results and Discussion. The sensitivity of SiNW FET nanosensor capable of sensing the presence of bound charged species by their intrinsic charge is critically dependent on their size and surface to volume ratio. For SiNW fabrication, the advent of the "top-down" method[15,38,39] has overcome the integration issues faced by the traditional "bottom-up" method. In this work, we developed a novel "top-down" method[24] by using complementary metal oxide semiconductor (CMOS) compatible technology including conventional optical lithography, anisotropic wet etching and so on for SiNW arrays fabrication.[40,41] The tetramethylammonium hydroxide (TMAH) etches Si (111) planes at ∼1/100 the rate of all other planes and thereby eliminates edge imperfections not aligned to this plane and a very smooth (111) plane can be formed. Since the dry oxidization of silicon down to the nanometer level is a self-limiting process[42,43] and the lateral etching rate is very slow, the width of SiNW is controllable and reproducible, which can be precisely controlled by controlling the etching time and using self-limiting oxidization. In addition, the slow etching, high-quality oxide and high-temperature annealing guarantee the low level of nanowire noise at the Si/SiO_2 interface. We finally obtained well-ordered, homogeneous and highly responsive SiNWs with triangle cross-section and high surface-to-volume ratio.

dx.doi.org/10.1021/nl401628y | Nano Lett. XXXX, XXX, XXX−XXX

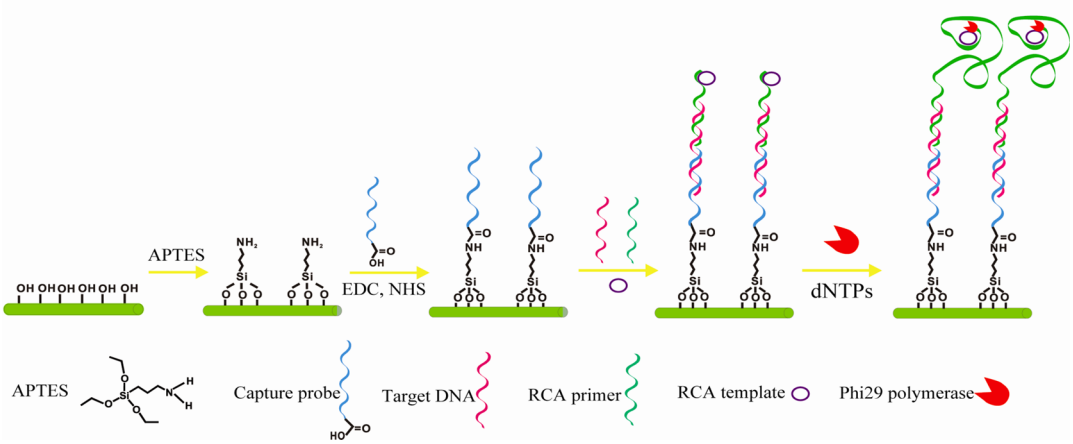

Figure 2. Schematic illustration of RCA-based SiNW detection of DNA.

Table 1. Sequence of Probe and Target Oligonucleotides

note	sequences (5′-3′)
capture probe	HOOC-TGGCTTTCAGTTATA
fully complementary target DNA	ATACCACATCATCCATATAACTGAAAGCCA
1-base mismatched target DNA	ATACCACATCATCCACATAACTGAAAGCCA
noncomplementary target DNA	GCCATCTATTGCCCAATCGGCTTAGCCATG
RCA primer	TGGATGATGTGGTATTTTTTTTTTTTTTTTCGTGTCCTCGTTGTCTGCTC
RCA template	GCTTTCGATCGTTCTGAGCAGACAACGAGGACACGCTTACTGAATAGCTA

The completed SiNW was configured as FET device including source, drain, and gate electrodes as illustrated in the schematic in Figure 1a. After the fabrication of SiNW and gold electrodes, a protective layer of silicon nitride was coated on the surface and only the silicon nanowire was exposed by a deep UV photolithographic process, while the oxide on the nanowire remained covered. This process allows the exposure of only the silicon nanowire to air/solution and thus increases sensitivity of the nanosensor.[44] The SiNW-FET based biosensor is a three-electrode system and two bias voltages are needed for sensing (Figure 1b). The function of the source/drain bias voltage is to bridge the semiconductor channel made of SiNWs and the gate potential is responsible for modulating the channel conductance. A scanning electron microscopy image of a representative SiNW is shown in Figure 1c. Owing to the planarization of the anisotropic wet etching, the nanowire has no much roughness.

To verify the quality of SiNWs, the source-drain current (I_{DS}) versus source-drain voltage (V_{DS}) dependence for varying gate-source voltage (V_{GS}) and the I_{DS}/V_{GS} curve for a constant voltage were measured prior to the surface modification of SiNW. The n-type, phosphorus-doped SiNW FETs were employed in this work. Generally, in the measurement of the I_{DS}/V_{DS} curve, the source-drain current was measured at several constant bias voltages (V_{GS} from −20 to 20 V with a step of 2 V) while sweeping the V_{DS} from −5 to 5 V to test the performance of SiNW FET. Also, in the measurement of the I_{DS}/V_{GS} curve I_{DS} was measured at constant voltage (V_{DS} = 1 V) while sweeping the gate potential (V_{GS}) from −20 to 20 V. As seen in Figure 1d, the I_{DS}/V_{DS} curve of the SiNW shows saturation asV_{DS} increased that yielded typical n-type accumulation mode behavior with a large on/off current ratio, I_{on}/I_{off}, exceeding 10^6. The I_{DS}/V_{GS} curve for V_{DS} = 1 V (Figure 1d, inset) helps to choose the sensing parameter for practical biochemical applications. Furthermore, our device shows very small electronic hysteresis between forward sweep and backward sweep, indicating a small density of trapped charges inside the structure (see Supporting Information Figure S1).[15]

We then employed the n-type SiNW-FET device to electrically detect HBV DNA through hybridization and RCA signal amplification. The schematic design of DNA detection with the combination of RCA and SiNW is shown in Figure 2. All DNA oligonucleotides used in this work are listed in Table 1. Capture probe DNA with the terminal carboxyl group was first conjugated to the amine of the 3-aminopropyltriethoxysilane (APTES)-modified SiNWs with the help of *N*-hydroxysuccinimide (NHS) and 1-ethyl-3-(3-dimethylaminopropyl) carbodiimide (EDC). The probe modification was followed by sandwich hybridization with the perfect matched target DNA and RCA primer. Afterward, the RCA template was hybridized to RCA primer after the 5′- and 3′- termini were joined by a DNA ligase.[32,45] Then, the RCA reaction was performed in the presence of the Phi29 DNA polymerase and dNTPs at room temperature, which created a long single-stranded DNA (ssDNA) product. Through RCA reaction, the signal of target DNA was significantly amplified, and the amplification efficiency correlated with the perfect matched target DNA concentration. The detailed process and parameters can be found in Experimental Section.

The change of SiNW characteristics after different treatments was studied and thus further elucidated the field-effect of the SiNWs. Upon exposure to different buffer solutions, the output I_{DS}/V_{DS} characteristic curves of the device were modified as shown in Figure 3a. The change with different solution that forms a different electrostatic charge environment of SiNW is crucial in explaining the behavior of the SiNW biomolecular sensor. Consequently, the electrostatic charges associated with the biomolecular reactions play the role of an effective gate voltage and the detection process does not introduce significant

dx.doi.org/10.1021/nl401628y | *Nano Lett.* XXXX, XXX, XXX−XXX

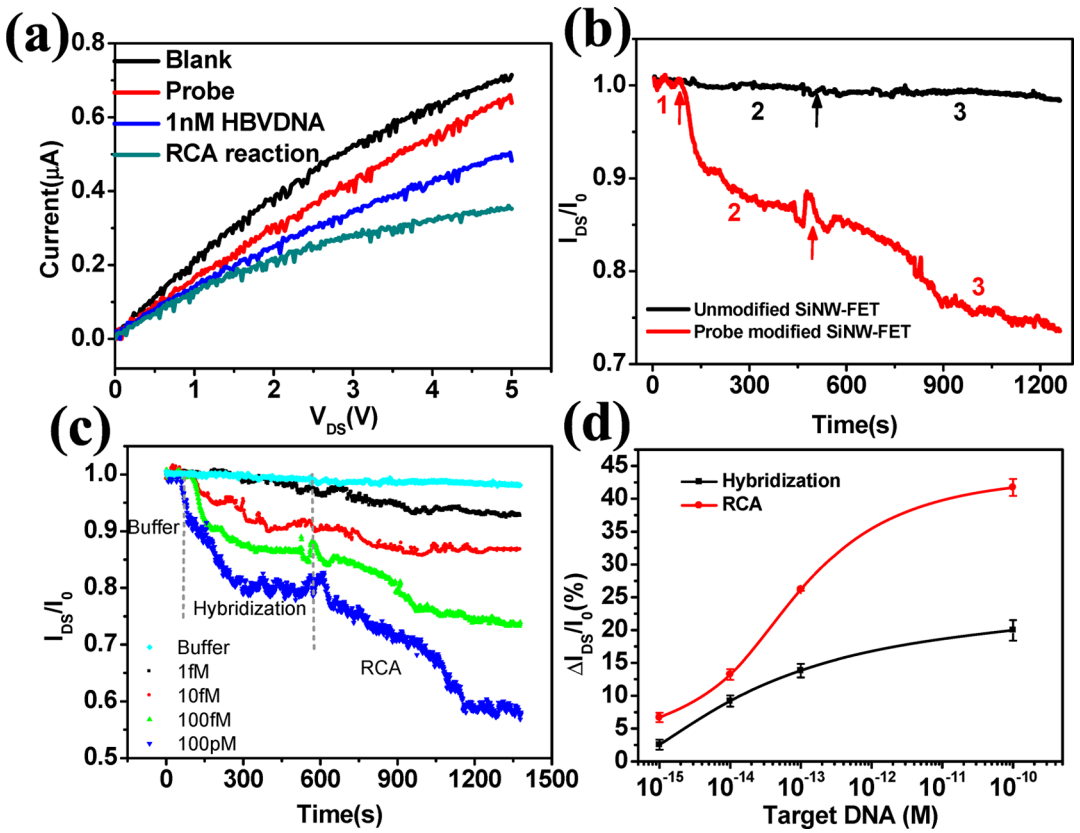

Figure 3. Enhanced DNA detection with RCA based on SiNWs. (a) The $I-V$ characteristics of the same SiNW when exposed to different solutions. (b) Plots of SiNW current versus time for a probe DNA-modified SiNW-FET and an unmodified SiNW-FET, where region 1 corresponds to the flow of hybridization buffer solution without target DNA, region 2 corresponds to the addition of 100 fM (red) and 1 pM (black) fully complementary target HBV DNA, and region 3 corresponds to the introduction of RCA solution. (c) Plots of normalized current change versus time with target HBV DNA at a series of concentrations (1 fM, 10 fM, 100 fM, and 100 pM) for probe DNA-modified SiNW device. (d) Relative current change ($\Delta I_{DS}/I_0$) as a function of the logarithm of target HBV DNA concentration for hybridization and RCA reaction process. I_0 represents the value of the initial current (t = 0). The length of SiNWs used in these studies was of 25 μm.

changes in the electronic structure of the nanowire. To avoid any influence of the pH in the measurements, the same pH = 7.4 has been used in all the measurements and solutions.

The DNA detection by real time monitoring the current change was explored. When the buffer solution (0.1×) flowed through the capture probe modified SiNW sensor surface, the electrical response of the SiNW-FET remained nearly unchanged. Significantly, when the hybridization solution containing 100 fM target DNA was introduced, the time-dependent current measurement exhibited a rapid current drop (Figure 3b). Of note, the decrease in electrical current coincides well with previous reports,[14,15,24,46] suggesting that the binding of negatively charged target DNA to the gate dielectric of n-type SiNW-FET results in the depletion of carriers.[47,48] The effect consistent with those previously noted[40,41] is essentially the mechanism of a semiconductor nanowire biosensor. A further current decrease of electrical current of SiNW observed after the addition of RCA reaction buffer was due to repeated sequences produced by RCA.[32,33] The greater number of sequences generated more negative charges on biosensor surface, acting as a negative gate that further depletes electron carriers in n-type nanowires and decreases the current. After the RCA amplification, the signal was significantly enhanced and the SNR of the SiNW device was improved by ∼100%. Significantly, unmodified SiNW exhibited very small current change after the 1 pM HBV DNA hybridization and RCA process (Figure 3b), which was comparatively negligible due to signal noise. The control experiment demonstrated that the observed results are due to specific target DNAs binding to the surface probes and the absence of nonspecific binding of target DNA to SiNW surface.

A further exploration of the detection ability and SNR improvement of the SiNW-RCA based biosensor was shown in Figure 3c, where target DNA in standard solution with a series of concentrations, ranging from 1 fM to 100 pM were tested. Solutions of DNA of various concentrations were prepared by dissolving and serially diluting DNA in 0.1× PBS as described in Experimental Section. Probe DNA-modified SiNW FET devices were used individually for different concentration DNA detection. The data was normalized by computing $|I_{DS}/I_0|$and plotted on the same axes for an effective comparison of the relative change in SiNW current at different concentrations of target DNA.

To evaluate the noise signal, blank buffer (0.1× PBS) without DNA was injected onto the SiNW surface, and the baseline was stabilized in the same buffer. As shown in Figure S2 (Supporting Information), the gate leakage current is very small, and similar $1/f$ noise power spectra of current have been explicitly in our nanowires. SiNWs are immune to large low-frequency $1/f$ noises that often plague conventional FETs as the dominant noise source.[49,50]

For a number of fluctuation noise, including correlated mobility fluctuations, the current noise power spectral density is given by[51−53]

dx.doi.org/10.1021/nl401628y | Nano Lett. XXXX, XXX, XXX−XXX

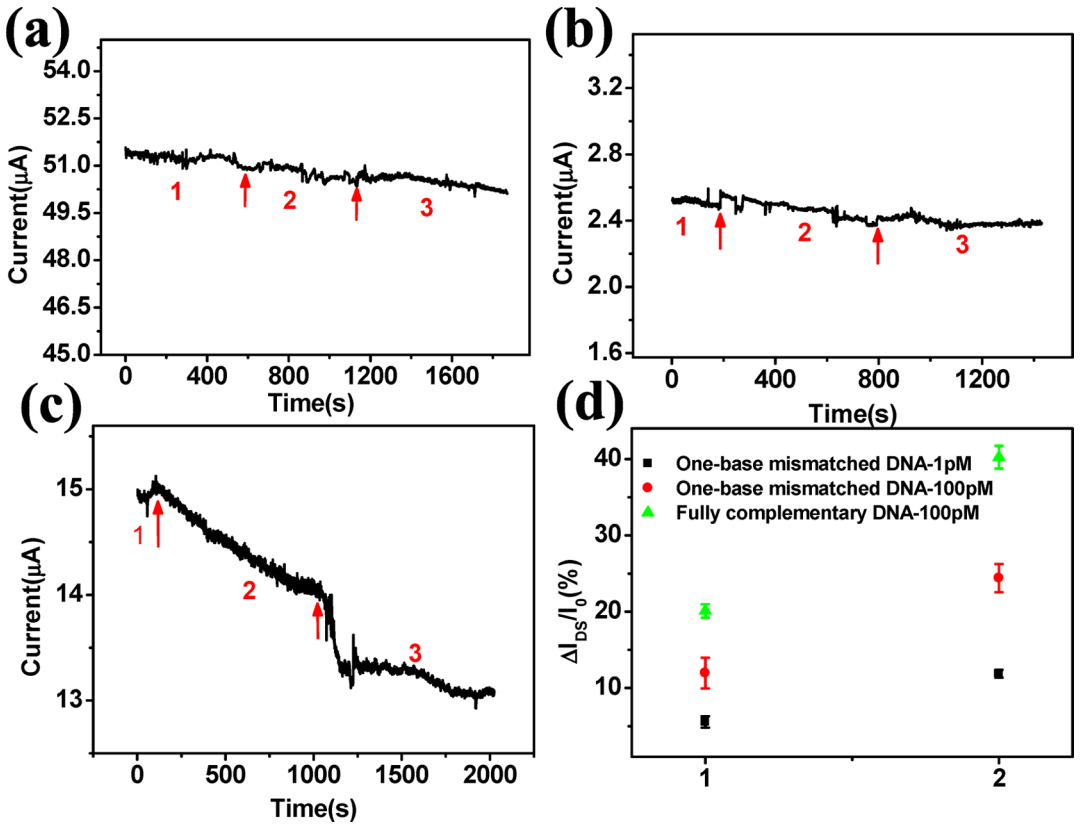

Figure 4. Specificity of SiNW biosensor. (a) Plot of current versus time for the modified SiNW-FET DNA sensor in absence of target HBV DNA, where region 1 stands for the flow of 0.1× PBS solution, region 2 for the addition of hybridization buffer solution without target DNA, and region 3 for the introduction of RCA solution. (b,c) Plots of current change of probe DNA modified SiNW-FET DNA sensor for noncomplementary DNA (b) and one-base mismatched HBV DNA (c), where region 1 corresponds to the flow of hybridization buffer solution, region 2 corresponds to the addition of 100 pM noncomplementary DNA (b) and 1 pM one-base mismatched target DNA (c), and region 3 corresponds to the introduction of RCA solution. (d) The normalized current change of SiNW biosensors after DNA hybridization and RCA reaction for 1 pM and 100 pM one-base mismatched target DNA detection and 100 pM fully complementary DNA detection. The length of SiNWs used in these studies was of 6 μm.

$$S_I = \left(1 + \alpha\mu C_{ox}\frac{I_{DS}}{g_m}\right)^2 g_m^2 \frac{\lambda kTq^2 N_t}{2\pi fRLC_{ox}^2} \quad (1)$$

where α is the Coulombic scattering coefficient, μ is the carrier mobility, C_{ox} is the oxide capacitance per unit area, g_m is transconductance, λ is the tunneling attenuation distance, k is the Boltzmann constant, and N_t is trap density. R and L are the SiNW radius and length, respectively

The root-mean-square (rms) current noise amplitude (δ_i) is obtained by integrating S_I over the measurement bandwidth and taking the square root ($\delta_i = (\int_{f_1}^{f_2} S_I df)^{1/2}$) and the measured signal response (ΔI) is given by the Supporting Information. Thus we arrive at the SNR which is given by

$$\mathrm{SNR} = \frac{\frac{\Delta I}{I_0}}{\frac{\delta_i}{I_0}} = \frac{2\pi RN_S}{\sqrt{\ln\left(\frac{f_2}{f_1}\right)}(Z + \alpha q\mu\pi R^2 n_0)}\sqrt{\frac{2\pi RL}{\lambda kTN_t}} \quad (2)$$

where N_S is surface density of bonded species number.

The expression gives the intrinsic SNR of SiNW FET and shows tunability of SNR by nanowire size and surface charges. The low-frequency noise originating from charge trapping/detrapping (N_t) and depending on the intrinsic device quality is the prevailing noise source in wet environments.[53] The noise-level dependency on ion concentration and pH level is negligible.[53−55] Therefore, a principal approach to achieve a higher SNR is the enrichment of surface charge density so as to unfreeze the severe limit of noise level to device sensitivity.

As shown in Figure 3c, concentration-dependent current changes were observed. The introduction of 1 fM, 10 fM, 100 fM, and 100 pM solutions of target DNA resulted in a current decrease of ∼2.5, ∼9, ∼14, and ∼20%, respectively. Notably, after the RCA reaction process, the SiNW current was significantly increased compared with that of introduction of target DNA. The current change of 1 fM, 10 fM, 100 fM, and 100 pM solutions of target DNA increased to ∼7, ∼13, ∼26, and ∼42%, respectively. RCA process made a great contribution to the change of SiNW current, which indicated a great potential to enhance the SNR of SiNW DNA biosensor. In theory, the greater the number of repeated sequences produced by RCA reaction, the greater the amount of the negative charge on biosensor surface, acting as gate voltage to charge SiNW FET. Therefore, a longer RCA reaction time was expected to generate more complementary segments of the circular template for enhanced signal amplification. It is drawn from Figure 3c that a stable SiNW current was obtained after some time when RCA reaction starts. We choose 1200−1300s as a stable region to calculate the device SNR, thus f_2 = 0.01 HZ, and f_1= 0.5 HZ. The current noise amplitude δ_i/I_0 is measured as 3.24×10^{-3} is buffer solution as shown in Figure. 3a. Therefore, the SNR of >20 was obtained for DNA concentration of 1 fM. Lieber's group has demonstrated that telomerase activity can be monitored down to 10 cell level

dx.doi.org/10.1021/nl401628y | Nano Lett. XXXX, XXX, XXX−XXX

without amplification and the detection of ~2 fM PSA was achieved with SNR >3.[14] Therefore, the enhanced SNR is much larger than previously reported,[14,56] implying a detection floor of 50 aM.[15] The parameter that also affects the device performance is Debye length,[44,57,58] the distance over which charge screen takes place. The surface density of bonded species affecting device SNR is directly proportional to the solution Debye screening length (see Supporting Information Equation S5). Therefore, the performance and SNR of the nanosensor can still be further improved by increasing the Debye length.

The response of SiNW after hybridization and RCA reaction process as a function of the log of DNA concentrations was illustrated in Figure 3d. Here, we define a relative suppression ratio of the current for the response of the device to the target DNA: $\Delta I/I_0$, where ΔI is the change of the current in the assay. The current of SiNW shift increases during the increase of target DNA concentrations, and RCA amplification work at all the concentrations. Compared with current change after DNA hybridization, the signal after RCA amplification increased more than 100%, implying a larger SNR and lower detection limit. The signal change of 1fM target DNA verified by the sensor response ~7% demonstrates the ultrahigh device sensitivity and effectiveness of RCA enhancement for this SiNW-FET sensor. This SNR should also be possible to be improved through variation in effective dopant concentration, improvements in the contacts, effective modification, reaction conditions and measuring techniques. Higher signal intensity through RCA amplification will lower the demands on the readout system. In addition, a high SNR is always an advantage because it will facilitate object analysis, reduce the number of false positive and false negative incidents, increase the multiplexing capability, and result in a more robust and portable protocol in general.

In addition, several control experiments were carried out to quantify any background effects due to the nonspecific binding and make sure the electronic responses of SiNW biosensor is caused by perfect complementary hybridization and RCA amplification. As shown in Figure 4a, the RCA reaction only leads to negligible current change in the absence of target HBV DNA with the exception of injection noise, which can be observed in all measurements of our experiments. After a stable reading was achieved in the hybridization buffer solution without target DNA (Figure 4b), the addition of 100 pM noncomplementary target DNA only produced a comparatively negligible change in current. Even the RCA reaction did not effectively lead to a significant current change. The specificity of the SiNW biosensor was further interrogated with one-base mismatched target DNA to demonstrate the reliability of RCA-based HBV DNA detection. The introduction of 1 pM one-base mismatched target DNA only leads to current change ~10% after RCA reaction, which is significantly lower than fully complementary target DNA (nearly 30%) (Figure 4c). We then extend the detection by evaluating the one-base mismatched target DNA of different concentrations. As shown in Figure 4d, the current change after DNA hybridization and RCA reaction for 1 pM and 100 pM one-base mismatched DNA and 100 pM fully complementary DNA was demonstrated. The concentration-dependent sensing results and the much smaller current change compared to fully complementary DNA further confirmed the specificity of SiNW biosensor. The controls show that there is little nonspecific binding of DNA on SiNW surface and only charges bounded on the SiNW surface is responsible for the current change. With sample enrichment by RCA, the interference from nonspecific binding onto the SiNW surface could be reduced substantially,[59] enhancing the specificity of SiNW device to some extent.

Conclusions. In conclusion, for the first time we have reported a label-free, ultrasensitive, electronic biosensor for HBV DNA detection based on a combination of CMOS-compatible SiNW FET and RCA amplification method. A CMOS-compatible anisotropic wet etching technique for the fabrication of SiNW arrays and a high-performance SiNW-FET biosensor has been developed. The SiNW-FET sensor demonstrated the ability to monitor HBV DNA hybridization and RCA reaction process and sense the response in real time. The biosensor has exhibited SNR > 20 for detection of 1 fM by employing the RCA amplification method, which exceeds the reported detection SNR by most previously reported DNA sensors.[14,56] This RCA-based SiNW biosensor also discriminated perfectly matched target DNA from 1-base mismatched DNA with high selectivity. The study could provide a guidance for the design and optimization of silicon nanowire sensor and the signal enhanced method should be especially useful in cases where the extrinsic noise level is high. Given the extraordinary ability for label-free and ultrasensitive biomolecure detection, mass reproducible ability, CMOS compatibility, as well as low cost character, the SiNW device was expected to provide a generic platform for numerous applications and offer great promise for early diagnosis of gene-related diseases.

Experimental Section. *Materials and Reagents.* All DNA oligonucleotides (Table 1) were purchased from Sangon Biotech Co., Ltd. (Shanghai, China). Phi29 DNA polymerase and Phi29 DNA polymerase reaction buffer were obtained from New England Biolabs. Bovine serum albumin (BSA) and deoxyribonucleoside 5′-triphosphates (dNTPs) mixture were obtained from Fermentas. The 3-aminopropyltriethoxysilane (APTES), phosphate-buffered saline (PBS), 1-ethyl-3-(3-(dimethylaminopropyl) carbodiimide (EDC), and *N*-hydroxysuccinimide (NHS) were purchased from Sigma-Aldrich (U.S.A.) and used as received. Other chemicals were obtained from Sinopharm Chemical Reagent Co., Ltd. (Shanghai, China). Solutions were prepared with Milli-Q deionized water.

SiNW Fabrication. Nanowire FET devices were fabricated from silicon-on-insulator (SOI) wafers as described previously in ref 38. Briefly, commercially available (100) oriented SIMOX silicon-on-insulator (SOI) wafers with light boron adulteration of 5×10^{15} cm^{-3} were used in this method. The NW-FET device regions were first defined with a wet chemical etch (tetramethylammonium hydroxide, TMAH), which etches Si(111) planes at ~1/100 the rate of all other planes. Then a thin nitride film (50 nm) was deposited by low-pressure-chemical-vapor-deposition (LPCVD) to protect the (111) plane previously defined. After the nitride film was patterned by ion-beam etching, the 100 nm SiO_2 layer beneath was totally removed by diluted HF. Then by using TMAH for the second time, we finally got controllable SiNW arrays with a triangular cross section after removing the nitride film. It should be noted that this etch produces triangular devices due to the (100) orientation of the SOI wafers. To decrease the density of surface dangling bonds on the Si surface and increase the stability of the sensors, a high-quality SiO_2 layer was finally thermally oxidized on the silicon nanowire surfaces.

Surface Modification. After the fabrication, the nanowires are functionalized by applying silanization. The SiNWs were first prepared by cleaning in an oxygen plasma (1.2 mbar, 150

dx.doi.org/10.1021/nl401628y | *Nano Lett.* XXXX, XXX, XXX–XXX

W for 600 s) to remove contaminates as well as to generate more hydrophilic surfaces with hydroxyl terminating the silicon-oxide surface. Then the devices were immerged in 2% absolute ethanol solution of APTES overnight, followed by rinsing thoroughly with ethanol. Following this, a self-assembled monolayer with terminal amino group was prepared by blowing the surface with nitrogen and heating at 120 °C for 5 min.

DNA Hybridization. For capture probe immobilization, 5′-carboxyl-modified single-stranded DNA (ssDNA) was modified on the surface of the silanized nanowires by exposing nanowire to PBS solution that contained 1 μM ssDNA, freshly prepared EDC (0.2 mM), and NHS (0.8 mM) solution for 3 h. For target DNA hybridization, the capture probe modified nanowires were immerged in 10 μL of hybridization solution containing 1 μL of perfect matched target DNA (1 fM ∼100 pM), 1 μM RCA primer, 0.1 × PBS, and 1 μM RCA template. After the incubation at room temperature for about 10 min, the nanowires were washed three times with buffer.

RCA Reaction. After DNA hybridization, RCA solution including Phi29 DNA polymerase (0.1 U/μL), Phi29 DNA polymerase reaction buffer (0.1 ×), dNTPs (1 mM for each of dATP, dCTP, dGTP and dTTP), and 1 mg/mL BSA were introduced onto surface of nanowires, and the reaction was carried out at room temperature. The real-time monitoring of the RCA process was carried out by observing current change of SiNW devices. After RCA reaction, the solution was removed from the surface of the nanowire.

Sensing Apparatus and Parameters. For general electrical measurement, SiNW was characterized by using a Cascade probe station with HP 4156 module, which can control gate potential and source/drain bias voltage. SiNW for real-time DNA sensing and RCA process monitoring was performed by using an Agilent 34410A multimeter.

■ ASSOCIATED CONTENT

Ⓢ Supporting Information

Sweep and noise property of SiNW FET, and theoretical analysis for signal response upon molecule bonded on nanowire surface. This material is available free of charge via the Internet at http://pubs.acs.org.

■ AUTHOR INFORMATION

Corresponding Author

*E-mail: (T.L) tli@mail.sim.ac.cn; (Y.W.) ylwang@mail.sim.ac.cn; (H.M.) hjmao@mail.sim.ac.cn. Fax: (+) 86-21-6213-1744; (+) 86-21-62511070-8714.

Author Contributions

†The first two authors, A.G., N.Z., contributed equally to this work.

Notes

The authors declare no competing financial interest.

■ ACKNOWLEDGMENTS

We appreciate financial support from National Basic Research Program of China (973 Program No. 2012CB933300, No. 2011CB309501), Creative Research of National Natural Science Foundation of China (No. 61021064), and the National Natural Science Foundation of China (No. 91123037, No. 60936001).

■ REFERENCES

(1) Risch, N.; Merikangas, K. The future of genetic studies of complex human diseases. *Science* **1996**, *273* (5281), 1516−1517.

(2) McCarthy, J. J.; Hilfiker, R. The use of single-nucleotide polymorphism maps in pharmacogenomics. *Nat. Biotechnol.* **2000**, *18* (5), 505−508.

(3) Bowtell, D. D. L. Options available - from start to finish - for obtaining expression data by microarray. *Nat. Genet.* **1999**, *21*, 25−32.

(4) Schena, M.; Shalon, D.; Davis, R. W.; Brown, P. O. Quantitative Monitoring of Gene-Expression Patterns with a Complementary-DNA Microarray. *Science* **1995**, *270* (5235), 467−470.

(5) Janasek, D.; Franzke, J.; Manz, A. Scaling and the design of miniaturized chemical-analysis systems. *Nature* **2006**, *442* (7101), 374−380.

(6) Nakamura, Y. The role of genetic diagnosis in clinics–from the choice of ordering until reading the data. *Rinsho byori. Jpn. J. Clin. Pathol.* **1999**, *47* (11), 1006.

(7) Burgess, D. C. H.; Wasserman, J.; Dahl, C. A. Global health diagnostics. *Nature* **2006**, *444*, 1−2.

(8) Dawson, E. D.; Moore, C. L.; Dankbar, D. M.; Mehlmann, M.; Townsend, M. B.; Smagala, J. A.; Smith, C. B.; Cox, N. J.; Kuchta, R. D.; Rowlen, K. L. Identification of A/H5N1 Influenza Viruses Using a Single Gene Diagnostic Microarray. *Anal. Chem.* **2007**, *79* (1), 378−384.

(9) Mao, H. L.; Wang, H. M.; Zhang, D. L.; Mao, H. J.; Zhao, J. L.; Shi, J.; Cui, Z. C. Study of hepatitis B virus gene mutations with enzymatic colorimetry-based DNA microarray. *Clin. Biochem.* **2006**, *39* (1), 67−73.

(10) Cha, B. H.; Lee, S. M.; Park, J. C.; Hwang, K. S.; Kim, S. K.; Lee, Y. S.; Ju, B. K.; Kim, T. S. Detection of Hepatitis B Virus (HBV) DNA at femtomolar concentrations using a silica nanoparticle-enhanced microcantilever sensor. *Biosens. Bioelectron.* **2009**, *25* (1), 130−135.

(11) Mirkin, C. A.; Letsinger, R. L.; Mucic, R. C.; Storhoff, J. J. A DNA-based method for rationally assembling nanoparticles into macroscopic materials. *Nature* **1996**, *382* (6592), 607−609.

(12) Wu, G. H.; Datar, R. H.; Hansen, K. M.; Thundat, T.; Cote, R. J.; Majumdar, A. Bioassay of prostate-specific antigen (PSA) using microcantilevers. *Nat. Biotechnol.* **2001**, *19* (9), 856−860.

(13) Chen, R. J.; Choi, H. C.; Bangsaruntip, S.; Yenilmez, E.; Tang, X. W.; Wang, Q.; Chang, Y. L.; Dai, H. J. An Investigation of the Mechanisms of Electronic Sensing of Protein Adsorption on Carbon Nanotube Devices. *J. Am. Chem. Soc.* **2004**, *126* (5), 1563−1568.

(14) Zheng, G. F.; Patolsky, F.; Cui, Y.; Wang, W. U.; Lieber, C. M. Multiplexed electrical detection of cancer markers with nanowire sensor arrays. *Nat. Biotechnol.* **2005**, *23* (10), 1294−1301.

(15) Stern, E.; Klemic, J. F.; Routenberg, D. A.; Wyrembak, P. N.; Turner-Evans, D. B.; Hamilton, A. D.; LaVan, D. A.; Fahmy, T. M.; Reed, M. A. Label-free immunodetection with CMOS-compatible semiconducting nanowires. *Nature* **2007**, *445* (7127), 519−522.

(16) Patolsky, F.; Zheng, G. F.; Hayden, O.; Lakadamyali, M.; Zhuang, X. W.; Lieber, C. M. Electrical detection of single viruses. *Proc. Natl. Acad. Sci. U.S.A.* **2004**, *101* (39), 14017−14022.

(17) Patolsky, F.; Zheng, G. F.; Lieber, C. M. Nanowire-Based Biosensors. *Anal. Chem.* **2006**, *78* (13), 4260−4269.

(18) Wang, W. U.; Chen, C.; Lin, K. H.; Fang, Y.; Lieber, C. M. Label-free detection of small-molecule-protein interactions by using nanowire nanosensors. *Proc. Natl. Acad. Sci. U.S.A.* **2005**, *102* (9), 3208−3212.

(19) Weissman, M. B. 1/F Noise and Other Slow, Nonexponential Kinetics in Condensed Matter. *Rev. Mod. Phys.* **1988**, *60* (2), 537−571.

(20) Zheng, G. F.; Gao, X. P. A.; Lieber, C. M. Frequency Domain Detection of Biomolecules Using Silicon Nanowire Biosensors. *Nano Lett.* **2010**, *10* (8), 3179−3183.

(21) Gao, X. P. A.; Zheng, G. F.; Lieber, C. M. Subthreshold Regime has the Optimal Sensitivity for Nanowire FET Biosensors. *Nano Lett.* **2010**, *10* (2), 547−552.

(22) Im, Y.; Lee, C.; Vasquez, R. P.; Bangar, M. A.; Myung, N. V.; Menke, E. J.; Penner, R. M.; Yun, M. H. Investigation of a single Pd nanowire for use as a hydrogen sensor. *Small* **2006**, *2* (3), 356−358.

(23) Hassibi, A.; Zahedi, S.; Navid, R.; Dutton, R. W.; Lee, T. H. Biological shot-noise and quantum-limited signal-to-noise ratio in affinity-based biosensors. *J. Appl. Phys.* **2005**, *97* (8), 084701−084701−10.
(24) Cui, Y.; Wei, Q. Q.; Park, H. K.; Lieber, C. M. Nanowire nanosensors for highly sensitive and selective detection of biological and chemical species. *Science* **2001**, *293* (5533), 1289−1292.
(25) Soleymani, L.; Fang, Z. C.; Sargent, E. H.; Kelley, S. O. Programming the detection limits of biosensors through controlled nanostructuring. *Nat. Nanotechnol.* **2009**, *4* (12), 844−848.
(26) Patolsky, F.; Lichtenstein, A.; Willner, I. Detection of Single-Base DNA Mutations by Enzyme-Amplified Electronic Transduction. *Nat. Biotechnol.* **2001**, *19*, 253−257.
(27) Polsky, R.; Gill, R.; Kaganovsky, L.; Willner, I. Nucleic Acid-Functionalized Pt Nanoparticles: A Catalytic Label for the Amplified Electrochemical Detection of Biomolecules. *Anal. Chem.* **2006**, *78*, 2268−2271.
(28) Li, D.; Yan, Y.; Wieckowska, A.; Willner, I. Amplified Electrochemical Detection of DNA through the Aggregation of Au Nanoparticles on Electrodes and the Incorporation of Methylene Blue into the DNA-Crosslinked Structure. *Chem. Commun.* **2007**, 3544−3546.
(29) Weizmann, Y.; Patolsky, F.; Katz, E.; Willner, I. Amplified DNA Sensing and Immunosensing by the Rotation of Functional Magnetic Particles. *J. Am. Chem. Soc.* **2003**, *125*, 3452−3454.
(30) Edwards, M. C.; Gibbs, R. A. Multiplex PCR - Advantages, Development, and Applications. *PCR Methods Appl.* **1994**, *3* (4), S65−S75.
(31) Phillips, J.; Eberwine, J. H.; Antisense, R. N. A. amplification: a linear amplification method for analyzing the mRNA population from single living cells. *Methods* **1996**, *10* (3), 283−288.
(32) Stromberg, M.; Goransson, J.; Gunnarsson, K.; Nilsson, M.; Svedlindh, P.; Stromme, M. Sensitive Molecular Diagnostics Using Volume-Amplified Magnetic Nanobeads. *Nano Lett.* **2008**, *8* (3), 816−821.
(33) Zhao, W.; Ali, M. M.; Brook, M. A.; Li, Y. Rolling circle amplification: applications in nanotechnology and biodetection with functional nucleic acids. *Angew. Chem., Int. Ed.* **2008**, *47* (34), 6330−6337.
(34) Korny, T.; Hayman, R. B.; Walt, D. R. Microsphere-based rolling circle amplification microarray for the detection of DNA and proteins in a single assay. *Anal. Chem.* **2009**, *81*, 5777−5782.
(35) Zhou, L.; Ou, L. J.; Chu, X.; Shen, G. L.; Yu, R. Q. Aptamer-Based Rolling Circle Amplification: A Platform for Electrochemical Detection of Protein. *Anal. Chem.* **2007**, *79*, 7492−7500.
(36) Zhang, S. B.; Wu, Z. S.; Shen, G. L.; Yu, R. Q. A label-free strategy for SNP detection with high fidelity and sensitivity based on ligation-rolling circle amplification and intercalating of methylene blue. *Biosens. Bioelectron* **2009**, *24*, 3201−3207.
(37) Cheng, Y. Q.; Zhang, X.; Li, Z. P.; Jiao, X. X.; Wang, Y. C.; Zhang, Y. L. Highly Sensitive Determination of microRNA Using Target-Primed and Branched Rolling-Circle Amplification. *Angew. Chem., Int. Ed.* **2009**, *48*, 3268−3272.
(38) Pui, T. S.; Agarwal, A.; Ye, F.; Balasubramanian, N.; Chen, P. CMOS-Compatible Nanowire Sensor Arrays for Detection of Cellular Bioelectricity. *Small* **2009**, *5* (2), 208−212.
(39) Li, Z.; Zhang, Y.; Fullhart, P.; Mirkin, C. A. Reversible and Chemically Programmable Micelle Assembly with DNA Block-Copolymer Amphiphiles. *Nano Lett.* **2004**, *4* (6), 1055−1058.
(40) Gao, A.; Lu, N.; Wang, Y.; Dai, P.; Li, T.; Gao, X.; Wang, Y.; Fan, C. Enhanced Sensing of Nucleic Acids with Silicon Nanowire Field Effect Transistor Biosensors. *Nano Lett.* **2012**, *12* (10), 5262−5268.
(41) Gao, A. R.; Lu, N.; Dai, P. F.; Li, T.; Pei, H.; Gao, X. L.; Gong, Y. B.; Wang, Y. L.; Fan, C. H. Silicon-Nanowire-Based CMOS-Compatible Field-Effect Transistor Nanosensors for Ultrasensitive Electrical Detection of Nucleic Acids. *Nano Lett.* **2011**, *11* (9), 3974−3978.
(42) Grydlik, M.; Brehm, M.; Hackl, F.; Groiss, H.; Fromherz, T.; Schäffler, F.; Bauer, G. Inverted Ge islands in {111} faceted Si pits—a novel approach towards SiGe islands with higher aspect ratio. *New J. Phys.* **2010**, *12* (6), 063002.
(43) Sievila, P.; Chekurov, N.; Tittonen, I. The fabrication of silicon nanostructures by focused-ion-beam implantation and TMAH wet etching. *Nanotechnology* **2010**, *21*, 14.
(44) Stern, E.; Wagner, R.; Sigworth, F. J.; Breaker, R.; Fahmy, T. M.; Reed, M. A. Importance of the Debye Screening Length on Nanowire Field Effect Transistor Sensors. *Nano Lett.* **2007**, *7* (11), 3405−3409.
(45) Li, J.; Zhong, W. Typing of Multiple Single-Nucleotide Polymorphisms by a Microsphere-Based Rolling Circle Amplification Assay. *Anal. Chem.* **2007**, *79* (23), 9030−9038.
(46) Hahm, J.-i.; Lieber, C. M. Direct Ultrasensitive Electrical Detection of DNA and DNA Sequence Variations Using Nanowire Nanosensors. *Nano Lett* **2004**, *4* (1), 51−54.
(47) Bergveld, P. Development, operation, and application of the ion-sensitive field-effect transistor as a tool for electrophysiology. *IEEE Trans. Biomed. Eng.* **1972**, *5*, 342−351.
(48) Turner, A. P.; Karube, I.; Wilson, G. S. *Biosensors: Fundamentals and Applications*; Oxford University Press: Oxford, 1987; p 21.
(49) Lin, Y. M.; Appenzeller, J.; Chen, Z. H.; Avouris, P. Electrical transport and 1/f noise in semiconducting carbon nanotubes. *Physica E* **2007**, *37* (1−2), 72−77.
(50) Voelker, M.; Fromherz, P. Signal transmission from individual mammalian nerve cell to field-effect transistor. *Small* **2005**, *1* (2), 206−210.
(51) Ghibaudo, G.; Roux, O.; Nguyenduc, C.; Balestra, F.; Brini, J. Improved Analysis of Low-Frequency Noise in Field-Effect Mos-Transistors. *Phys. Status Solidi A* **1991**, *124* (2), 571−581.
(52) Jayaraman, R.; Sodini, C. G. A 1/F Noise Technique to Extract the Oxide Trap Density near the Conduction-Band Edge of Silicon. *IEEE Trans. Electron Devices* **1989**, *36* (9), 1773−1782.
(53) Rajan, N. K.; Routenberg, D. A.; Reed, M. A. Optimal signal-to-noise ratio for silicon nanowire biochemical sensors. *Appl. Phys. Lett.* **2011**, *98*, 264107.
(54) Kim, S.; Rim, T.; Kim, K.; Lee, U.; Baek, E.; Lee, H.; Baek, C. K.; Meyyappan, M.; Deen, M. J.; Lee, J. S. Silicon nanowire ion sensitive field effect transistor with integrated Ag/AgCl electrode: pH sensing and noise characteristics. *Analyst* **2011**, *136* (23), 5012−5016.
(55) Clément, N.; Nishiguchi, K.; Dufreche, J.; Guerin, D.; Fujiwara, A.; Vuillaume, D. A silicon nanowire ion-sensitive field-effect transistor with elementary charge sensitivity. *Appl. Phys. Lett.* **2011**, *98* (1), 014104−014104−3.
(56) Agarwal, A.; Buddharaju, K.; Lao, I. K.; Singh, N.; Balasubramanian, N.; Kwong, D. L. Silicon nanowire sensor array using top-down CMOS technology. *Sens. Actuators, A* **2008**, *145*, 207−213.
(57) Sorensen, M. H.; Mortensen, N. A.; Brandbyge, M. Screening model for nanowire surface-charge sensors in liquid. *Appl. Phys. Lett.* **2007**, *91*, 102105.
(58) De Vico, L.; Sorensen, M. H.; Iversen, L.; Rogers, D. M.; Sorensen, B. S.; Brandbyge, M.; Nygard, J.; Martinez, K. L.; Jensen, J. H. Quantifying signal changes in nano-wire based biosensors. *Nanoscale* **2011**, *3* (2), 706−717.
(59) Kao, L. T.-H.; Shankar, L.; Kang, T. G.; Zhang, G.; Tay, G. K. I.; Rafei, S. R. M.; Lee, C. W. H. Multiplexed detection and differentiation of the DNA strains for influenza A (H1N1 2009) using a silicon-based microfluidic system. *Biosens. Bioelectron.* **2011**, *26* (5), 2006−2011.